Journal of Environmental Radioactivity 268-269 (2023) 107260

Contents lists available at ScienceDirect

Journal of Environmental Radioactivity

journal homepage: www.elsevier.com/locate/jenvrad

Chemical availability of fallout radionuclides in cryoconite

H. Davidson [a], G.E. Millward [a], C.C. Clason [b,*], A. Fisher [a], A. Taylor [a]

[a] School of Geography, Earth and Environmental Sciences, University of Plymouth, Plymouth, UK
[b] Department of Geography, Durham University, Durham, UK

ARTICLE INFO

Keywords:
Fallout radionuclides
Cryoconite
Glaciers
Contaminant mobility
Sequential extractions
Chemical availability

ABSTRACT

Atmospheric deposition on glaciers is a major source of legacy fallout radionuclides (FRNs) accumulating in cryoconite, a dark granular material with surface properties that efficiently bind FRN contaminants (specifically ^{137}Cs; ^{210}Pb; ^{241}Am). Cryoconite-bound FRNs in glaciers can be released when they interact with and are transported by glacial meltwater, resulting in the discharge of amassed particulate contaminants into aquatic and terrestrial environments downstream. The environmental consequences of FRN release from the cryosphere are poorly understood, including impacts of cryoconite-sourced FRNs for alpine food chains. Consequently, there is limited understanding of potential health risks to humans and animals associated with the consumption of radiologically-contaminated meltwater. To assess the chemical availability of cryoconite-adsorbed FRNs we used a three-stage sequential chemical extraction method, applied to cryoconite samples from glaciers in Sweden and Iceland, with original FRN activity concentrations up to 3300 Bq kg^{-1} for ^{137}Cs, 10,950 Bq kg^{-1} for unsupported ^{210}Pb (^{210}Pb$_{un}$) and 24.1 Bq kg^{-1} for ^{241}Am, and orders of magnitude above regional backgrounds. Our results demonstrate that FRNs attached to cryoconite are solubilized to different degrees, resulting in a stage-wise release of ^{210}Pb$_{un}$ involving significant stepwise solubilization, while ^{137}Cs and ^{241}Am tend to be retained more in the particulate phase. This work provides an insight into the vulnerability of pristine glacial environments to the mobilization of FRN-contaminated particles released during glacier melting, and their potential impact on glacial-dependent ecology.

1. Introduction

Glaciers are retreating rapidly in many regions across the globe in response to climate change, thereby accelerating the transport of meltwater and sediment deposits to downstream proglacial environments (Cauvy-Fraunié and Dangles, 2019; Milner et al., 2017). Recent studies show that glaciers and snowpacks in alpine regions can contain contaminants (Beard et al., 2022a, 2022b) such as persistent organic pollutants (e.g. Ferrario et al., 2017), microplastics (e.g. Stefánsson et al., 2021), and fallout radionuclides (FRNs) (e.g. Lokas et al., 2022; Clason et al., 2023). FRN contamination has risen in the Northern Hemisphere as a result of anthropogenic activities, including weapons testing, nuclear accidents, and developments of nuclear energy (Gadd, 1996; Mietelski, 2002). Contaminants deposited on glacier surfaces originate, to a significant extent, from remote sources, and predominantly via atmospheric transport (Corcho Alvarado et al., 2014). Snow is also an efficient scavenger of contaminants from the atmosphere (Franz and Eisenreich, 1998; Herbert et al., 2006), and some anthropogenic substances have been shown to preferentially accumulate in polar and alpine environments (Grannas et al., 2013). Consequently, many contaminants are detected at higher concentrations in ice, snow, and meltwater than in non-glaciated regions (Pawlak et al., 2021).

Cryoconite is a dark granular material that tends to accumulate in melt holes in the ablation zones of glacier surfaces (Cook et al., 2016). These cryoconite deposits can have a high biodiversity (Zawierucha et al., 2017) and have been shown to play an important role in nutrient cycling (Bagshaw et al., 2013). Cryoconite containing the artificially-produced FRNs ^{137}Cs and ^{241}Am, as well as natural and man-made ^{210}Pb$_{un}$, has been discovered across the global cryosphere (Clason et al., 2023), including sites in both the northern (Tieber et al., 2009; Baccolo et al., 2020a, 2020b; Wilflinger et al., 2018; Owens et al., 2019; Clason et al., 2021; Jiao et al., 2023) and southern (Buda et al., 2020; Owens et al., 2023) hemispheres. For example, Tieber et al. (2009) examined glaciers in the Northern Calcareous Alps, Austria, where cryoconite had elevated activities of ^{137}Cs and ^{241}Am in the ranges 1744–140,051 Bq kg^{-1} and <2.2–93.6 Bq kg^{-1}, respectively.

* Corresponding author.
E-mail address: caroline.clason@durham.ac.uk (C.C. Clason).

https://doi.org/10.1016/j.jenvrad.2023.107260
Received 19 May 2023; Received in revised form 19 July 2023; Accepted 21 July 2023
Available online 1 August 2023

Significant activity concentrations of FRNs have also been found in suspended sediments from the proglacial waters of a Canadian glacier (Owens et al., 2019) and in sediments from a glacier forefield in Arctic Sweden (Clason et al., 2021), but at orders of magnitude less than found in cryoconite at these sites. Thus, cryoconite has a unique ability to accumulate FRNs at levels significantly higher than those found in off-ice sediments. While there is an understanding of levels of FRN activity in cryoconite, their potential for chemical remobilisation within the glacial landscape remains poorly understood.

The accumulation of radionuclides by cryoconite creates a temporary particulate reservoir of FRNs because subsequent glacier retreat may stimulate the mobilization of the FRN-tagged cryoconite. This remobilisation results in downstream migration into proglacial meltwaters and freshwater ecosystems (Smith, 1978; Milner et al., 2017). However, several factors could influence the redistribution of FRNs, for example glacier hypsometry and local topography, meltwater residence time, and the meltwater flux as a proportion of total water discharge within the catchment (Huss and Hock, 2018). The interaction of cryoconite with meltwater in the supraglacial environment, and whether cryoconite deposits are 'wet' or 'dry', is also an important control on its ability to accumulate radionuclides (Ferrario et al., 2017; Owens et al., 2019; Baccolo et al., 2020a, 2020b). Regular interaction with meltwater increases the opportunity for legacy FRNs encapsulated in cryoconite to be released to the dissolved phase. However, to date, research monitoring particulate FRNs in cryoconite has been concerned with assessing accumulated total FRN activities rather than their potential for release from the particulate phase. Thus, the extent to which FRN remobilisation from cryoconite will occur within the context of radionuclide availability in the glacial environment requires further examination. The uptake of FRNs onto cryoconite may involve different geochemical phases, and an operationally-defined contaminant binding to particulate phases has been achieved using chemical sequential extraction procedures (Kenna, 2009; Taylor et al., 2012; Skipperud and Salbu, 2015).

In this work, selected cryoconite samples from two glaciated regions in the northern hemisphere are used to examine the chemical extractability of particulate radionuclides and assess the potential for their remobilisation. The intention here is to improve the understanding of environmental risk from cryoconite mobilization under future glacier retreat, particularly from potential release of sorbed radionuclides, and their dispersion within glacial aquatic systems. In this context, the objectives of our study are to: (1) determine the activity concentrations of FRNs found in cryoconite from Isfallsglaciären, Sweden and Skaftafellsjökull, Iceland; (2) assess the potential desorption of FRNs from cryoconite using sequential chemical extractions; and (3) improve the understanding of whether elevated levels of chemically-desorbable FRNs in cryoconite pose a potential threat to human and ecosystem communities in glacial regions.

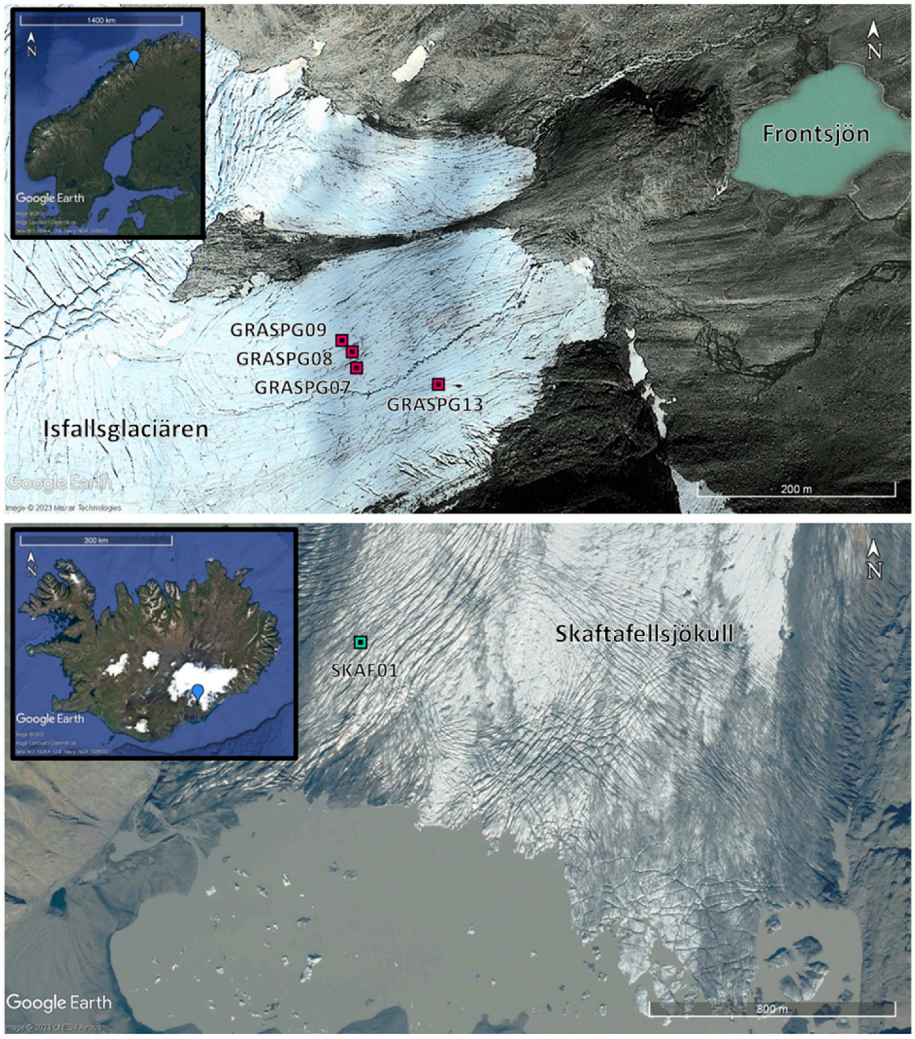

Fig. 1. Cryoconite sampling locations on Isfallsglaciären, Sweden (top panel) and Skaftafellsjökull, Iceland (bottom panel).

2. Study sites

The cryoconite samples discussed here were collected from sites in Sweden (Clason et al., 2021) and Iceland (unpublished). Four samples were collected at elevations between 1309 and 1330 m.a.s.l. on Isfallsglaciären in the Tarfala Valley of Arctic Sweden in August 2017 (Fig. 1). Isfallsglaciären is a small polythermal glacier which retreated between 1916 and 1990 at a rate of ~4 m a^{-1}. Since then, it has maintained its terminus position, with meltwater and sediments being released and transported into two proglacial lakes, Frontsjön and Isfallssjön, both situated within 700 m of the present-day glacier terminus. Arctic Sweden is known to have been a sink for radioactive fallout from the Chernobyl nuclear accident in 1986 (Åhman and Åhman, 1994; Skuterud et al., 2004), and is thus a useful site for examination of the contaminant concentrations and potential mobility of glacial sediments. The other sample we discuss here was collected in July 2018 at 248 m.a.s.l. on Skaftafellsjökull, an outlet glacier of Iceland's biggest ice cap, Vatnajökull. Skaftafellsjökull has undergone consistent retreat over recent decades, averaging 53 m a^{-1} since 1999, with associated impacts for downstream proglacial hydrology (Marren and Toomath, 2014). The mass of cryoconite in additional samples collected in Iceland was not sufficient for sequential extractions.

3. Methods

3.1. Sample collection and preparation

Four cryoconite samples from Isfallsglaciären were collected on-site using a spatially-integrated approach, whereby sufficient cryoconite was collected close to a central sampling point (Clason et al., 2021). A plastic spatula was used for cryoconite deposits accessible on ice surfaces and a pipette where cryoconite was submerged underwater. Samples were stored in cleaned plastic 50 ml tubes. The samples comprised heterogeneous mixtures of organic and inorganic components and were preserved by oven drying at 100 °C, to a constant weight, on site at Tarfala Research Station. The sample from Skaftafellsjökull was sampled following the procedure above, however, due to a lack of drying facilities on-site this sample was transported to the UK in an air-tight plastic tube and then freeze-dried prior to geochemical analysis.

3.2. Experimental strategy

To assess the potential chemical availability of FRNs in cryoconite the BCR (Community Bureau of Reference) three-step sequential extraction procedure was used, and the quantities of samples and reagents were similar to those specified (Pueyo et al., 2001). The concept behind sequential extraction is that desorption of the readily exchangeable FRNs occurs in the first extraction step, followed by the procedure progressively targeting more strongly held radionuclides in turn (Skipperud and Salbu, 2015). In our experiments acid-cleaned 50 ml polypropylene centrifuge tubes were used to hold the solid samples (2 g) which could be placed on a planar gamma counter allowing quantification of the activities of the solid for each extraction stage. The liquid extracts, i.e. the supernatants, were retained and counted separately in plastic containers of 100 ml volume. To validate the results of sequential extractions of cryoconite samples, as described below, the digest procedure was applied to the Certified Reference Material (CRM) BCR 701 and the elemental content for each extraction stage was determined. The results are shown in Table S1 of the Supplementary Materials.

3.3. Sequential extraction procedure

3.3.1. Stage 1 exchangeable fraction

This fraction is extracted using Solution A: 0.11 mol L^{-1} acetic acid made up in graduated polypropylene bottles. 40 ml of Solution A was added to each of five dry cryoconite samples, contained in centrifuge tubes, which were then shaken end-over-end continuously for 16 h at room temperature. Subsequently, the suspensions were centrifuged at 3000 rpm for 20 min after which the supernatants were carefully removed by pipette and stored in plastic containers, prior to gamma counting. The solid residues were washed with 20 ml of ultra-pure water, shaken for 15 min, followed by centrifugation. The supernatants were carefully removed by pipette, followed by drying and re-weighing of the solid phase. The weights of dried solids were close to the originals, with no more than 5% loss between stages. The activity concentrations of the solids, and liquid extracts, were determined by gamma spectrometry (described below).

3.3.2. Stage 2 reducible fraction

This fraction is extracted using Solution B: 0.5 mol L^{-1} hydroxylammonium chloride made up in a 1 L volumetric flask. 40 ml of freshly prepared Solution B was added to the dry solid residue remaining from Stage 1 and shaken at 150 rpm for 16 h at room temperature. Subsequently, each sample was separated from the supernatant by centrifugation at 3000 rpm for 20 min and the liquid phase was removed by pipette and stored in a plastic container. Solid residues were rinsed with 20 ml of ultra-pure water, shaken for 15 min, followed by centrifugation for 20 min at 3000 rpm. The supernatant was discarded, the solids dried, and their activity concentrations determined, as were those of the liquid extracts.

3.3.3. Stage 3 oxidisable fraction

This fraction is extracted using Solution C: 8.8 mol L^{-1} hydrogen peroxide, acid stabilised to pH = 2–3 and Solution D: 1.0 mol L^{-1} ammonium acetate in 1 L volumetric flask at pH = 2 adjusted with concentrated HNO_3. The extractions involved two solutions namely C and D which were added, in turn, to the dry solid residue remaining from Stage 2. 10 ml of solution C were slowly added, using a pipette, to the solid phase in each centrifuge tube. The stable suspensions were shaken for 1 h at room temperature after which the centrifuge tubes were placed in a water bath at 85 ± 2° for 1 h, with occasional shaking. The tubes were then uncovered and the volume of liquid in the samples allowed to reduce to ~3 ml by continual heating. The process was repeated by adding another 10 ml of solution C followed by heating of the tubes at 85 ± 2° and the solution left to react for 1 h. Sporadic manual shaking of the samples took place within the first 30 min, after which the covers were removed and the volumes reduced to ~1 ml. The tubes were monitored to prevent complete dryness. 50 ml of solution D was added to each of the tubes, which were then shaken for 16 h at room temperature. Afterwards, the extracts were separated from the solids by centrifugation and the liquids were decanted into plastic containers. The dried solid residues were rinsed with Milli-Q water, dried, and retained to determine the activity concentrations of FRNs in the solid samples by gamma counting.

3.3.4. Stage 4 residual fraction

Dried samples from Stage 3 were carefully transferred each to a cleaned conical flask and treated with 2 ml of Milli-Q water to create a slurry. 10 ml of concentrated *aqua regia* was added, and the samples shaken for 24 h at room temperature. The liquids and solids were separated by centrifugation, and after drying they were gamma counted.

3.4. Gamma spectrometry

Analyses of the radioactive standards and samples were carried out in the ISO9001-accredited Consolidated Radio-isotope Facility (CoRiF) at the University of Plymouth applying an established methodology. Gamma counting was conducted using a planar (GEM-FX8530-S; N-type) spectrometer, consisting of liquid nitrogen cooled, high purity germanium semiconductor detectors (EG&G ORTEC, Wokingham, UK). The planar detector had a full width-half maximum for the 1332 keV line

of ^{60}Co of 1.76 keV and a relative efficiency of 50.9%. The energy, peak width and efficiency of the gamma spectrometer was calibrated for liquids by using a 40 ml of water spiked with a certified, traceable mixed radioactive solution (80717-669 supplied by Eckert & Ziegler Analytics, Georgia, USA). The gamma detector was calibrated for activities in the solid phases using a natural, homogenized soil, with low background activity, which had been spiked with the certified, traceable mixed radioactive solution above. The counting of the solids, and the calibration standard, were carried out on 2 g of calibrant in sealed 50 ml plastic centrifuge tubes and the liquid phase calibrant was counted in 100 ml plastic containers. Counting was carried out for at least 48 h. Calibration relationships were derived using ORTEC GammaVision© software and all activities were decay corrected to the sample collection date. The uncertainties were estimated from the counting statistics and are quoted at the 2-sigma level. We report unsupported ^{210}Pb ($^{210}Pb_{un}$) activities here, which were obtained by the subtraction of ^{226}Ra activity, deduced from the gamma emissions of ^{214}Pb, from the measured total activity of ^{210}Pb. Quality control analyses were carried out using soils from the IAEA proficiency tests, including a moss soil (IAEA-CU-2009-03) and a soil (IAEA-TEL-2012-03) (Table S2 in Supplementary Materials).The minimum detectable activities (MDA) for the radionuclides determined in this study depended on sample and detector conditions where the values were ^{241}Am<1.0 Bq kg^{-1}, ^{137}Cs < 1,0 Bq kg^{-1} ^{214}Pb < 2.0 Bq kg-1 and ^{210}Pb < 5.0 Bq kg^{-1}.

3.5. Elemental analysis

The elemental composition of the samples was determined by Wavelength Dispersive X-ray Fluorescence (WD-XRF) spectrometry, while stable isotope analysis also conducted for the four Swedish samples (see Clason et al., 2021, for further details). Dried cryoconite samples were powdered by hand using a pestle and mortar prior to being packed into 40 mm diameter cups fitted with 6 μm polypropylene spectromembrane (Chemplex, USA). All samples were packed to the same volume and left to settle for 24 h prior to analysis. Analyses were undertaken in CoRiF by WD-XRF spectrometry (Axios Max, PANalytical, Netherlands). The instrument was operated at 4 kW using a Rh target X-ray tube. During sequential analysis of elements tube settings ranged from 25 kV, 160 mA for low atomic weight elements up to 60 kV, 66 mA for higher atomic weight elements. All analyses were undertaken using the Omnian analysis application (PANalytical, Netherlands) under a medium of He. Repeatability of the approach was assessed by repacking and analysing cryoconite samples in triplicate with relative standard deviation found to be <10% across triplicates. This procedure has been validated by Clason et al. (2021) whereby cross comparison to results obtained from a validated inductively coupled plasma optical emission spectrometry (ICP-OES) procedure showed XRF-derived concentrations were in close agreement (within 15% relative to ICP-OES) for the elements of interest.

4. Results

4.1. Elemental composition of cryoconite

The concentrations of selected elements in the cryoconite samples - prior to sequential extraction - are shown in Table 1, along with the background values for elemental concentrations in the upper continental crust (Wedepohl, 1995). The cryoconite samples from Sweden have elevated metal concentrations, and Cr, Pb and Cu have concentrations significantly above the probable effect level (PEL).

Enrichment Factors (EF) were estimated using Equation (1):

$$EF = \frac{\frac{(M)}{(Al)}}{\frac{(M)_{Ref}}{(Al)_{Ref}}} \quad (1)$$

where *(M)* is the total concentration of a metal, *(Al)* the total concentration of aluminium, and $(M)_{Ref}$ and $(Al)_{Ref}$ are the total concentrations of the metal and aluminium in the reference sediments taken as metal concentrations of sediments from the upper continental crust (Wedepohl, 1995). The ranges of EF (Table 2) are $1 < EF < 3$ which specifies minor enrichment, $3 < EF < 5$ which specifies moderate enrichment, $5 < EF < 10$ which specifies moderate to severe enrichment, and $EF > 10$ which is classed as severe enrichment. Estimates of EFs indicate that the samples from Sweden had severe enrichment of Pb and Cu, moderate to severe enrichment of Cr, Zn and Ni, and minor enrichment of Ti and Fe. While there is severe enrichment of Pb in Swedish cryoconites, the sample from Iceland had only moderate enrichment, and a trend of lower enrichment for this sample was observed for all elements apart from Ti (Table 2).

The percentages of carbon and nitrogen in the Swedish cryoconite samples, and their ratios, are shown in Table 3. The relatively low C/N ratio indicates a production of N from mineralization which may be released for uptake by flora or microorganisms in cryoconite (Zawierucha et al., 2017).

4.2. Activity concentrations of FRNs

Analysis of FRN concentrations in cryoconites revealed distinctly different results between the sites. The original activity concentrations, prior to the sequential extraction procedure, are displayed in Table 4. The samples from Isfallsglaciären have relatively high activity

Table 2
Enrichment factors for cryoconite samples.

Sample	Enrichment Factors						
	Cr	Pb	Cu	Zn	Ni	Ti	Fe
GRASPG07	6.9	25.2	13	4.3	11.2	3.5	3.5
GRASPG08	8.2	22.9	15.6	4.1	9.1	3.2	3.2
GRASPG09	10.2	19.2	12.1	4.4	8.7	3.2	3.3
GRASPG13	7.7	13.5	12.6	3.2	8.6	3.1	3.0
SKAF01	1.7	4.4	8.8	2.9	4.6	6.0	1.9

Table 1
Elemental concentrations of cryoconite (mg kg^{-1} dry weight) from Isfallsglaciären, Sweden (GRASPGXX) and Skaftafellsjökull, Iceland (SKAF01).

Sample	Elemental Concentrations, mg kg^{-1}							
	Al_2O_3	Al	Cr	Pb	Cu	Zn	Ni	Ti
GRASPG07	105000	54600	169	301	131	156	146	7580
GRASPG08	113000	58800	218	296	170	161	129	7670
GRASPG09	114000	59300	273	248	132	176	123	7620
GRASPG13	119000	61900	217	184	144	133	128	7810
SKAF01	144000	74880	57.2	71.8	122	145	81.9	18200
Continental Crust	–	77440	35.0	17.0	14.3	52.0	18.6	3117
PEL[a]	–	–	160	112	108	271	–	–

[a] PEL = Concentration above which adverse effects frequently occur (CCME, 1995).

Table 3
Carbon and nitrogen analyses for cryoconite samples from Isfallsglaciären.

Sample	Carbon and Nitrogen		
	% N	% C	C/N
GRASPG07	1.12	12.4	11.1
GRASPG08	0.99	11.5	11.6
GRASPG09	0.93	10.7	11.5
GRASPG13	1.18	12.0	10.2

Table 4
Original activity concentrations and counting errors (±2σ) of ^{137}Cs, ^{210}Pb$_{un}$ and ^{241}Am in natural cryoconite samples from Sweden and Iceland.

Sample	Activity Concentrations ± 2σ, Bq kg^{-1}		
	^{137}Cs	^{210}Pb$_{un}$	^{241}Am
GRASPG07	2890 ± 220	10950 ± 880	21.5 ± 7.6
GRASPG08	3300 ± 260	10540 ± 850	24.1 ± 7.4
GRASPG09	2420 ± 190	9620 ± 770	12.6 ± 6.7
GRASPG13	2830 ± 220	8880 ± 720	20.4 ± 8.9
SKAF01	174 ± 16	939 ± 113	6.2 ± 5.7

concentrations, with the maximum activities for artificial FRNs ^{137}Cs and ^{241}Am being recorded for GRASPG08. The Isfallsglaciären samples had original activity concentrations of ^{210}Pb$_{un}$ in excess of 8800 Bq kg-1 (Table 4), with lower but still relatively high activities of ^{137}Cs and ^{241}Am, i.e. >2400 Bq kg^{-1} and >12.6 Bq kg^{-1}, respectively, which are elevated significantly above background values (see Clason et al., 2021 for FRN activities in proglacial sediments). The activities of FRNs in all the Swedish samples were more than an order of magnitude higher than for the Skaftafellsjökull (SKAF01) sample, for which the highest activity recorded was for ^{210}Pb$_{un}$ (940 Bq kg^{-1}).

4.3. Sequential extractions

The three-stage extraction procedure was specifically designed to establish the fractions of contaminants in the various particulate compartments (Pueyo et al., 2001). The approach is supported by the creation of a certified reference soil (BCR 701) that has values with which our data coheres (Table S1 in Supplementary Materials) and the mass balances are given in Fig. S1 (Supplementary Materials). The results of the three-stage sequential extractions, and the fourth stage involving the concentrated acid extraction of residual components, are shown in Fig. 2. The majority of ^{210}Pb$_{un}$ in the cryoconite sediments was extracted in the reducible phase (Stage 2) with an average percentage loss of ~60% across the samples (Fig. 2; Table S3 in Supplementary materials). For ^{137}Cs there are only minor releases in stages 1, 2 and 3, with a significant quantity remaining in the residual phase, possibly due to ^{137}Cs being bound within the crystalline structures of primary and secondary minerals. The sequential extractions influenced ^{241}Am activity concentrations such that there was a ~20% loss in the initial exchangeable stage of the extractions for Swedish samples. In contrast, the sample from Iceland had no exchangeable ^{241}Am, suggesting that the isotopes are strongly bound and chemically stable. Most ^{241}Am activity was lost in the oxidisable fraction for this sample, which contrasts with both ^{137}Cs and ^{210}Pb$_{un}$ for the same sample.

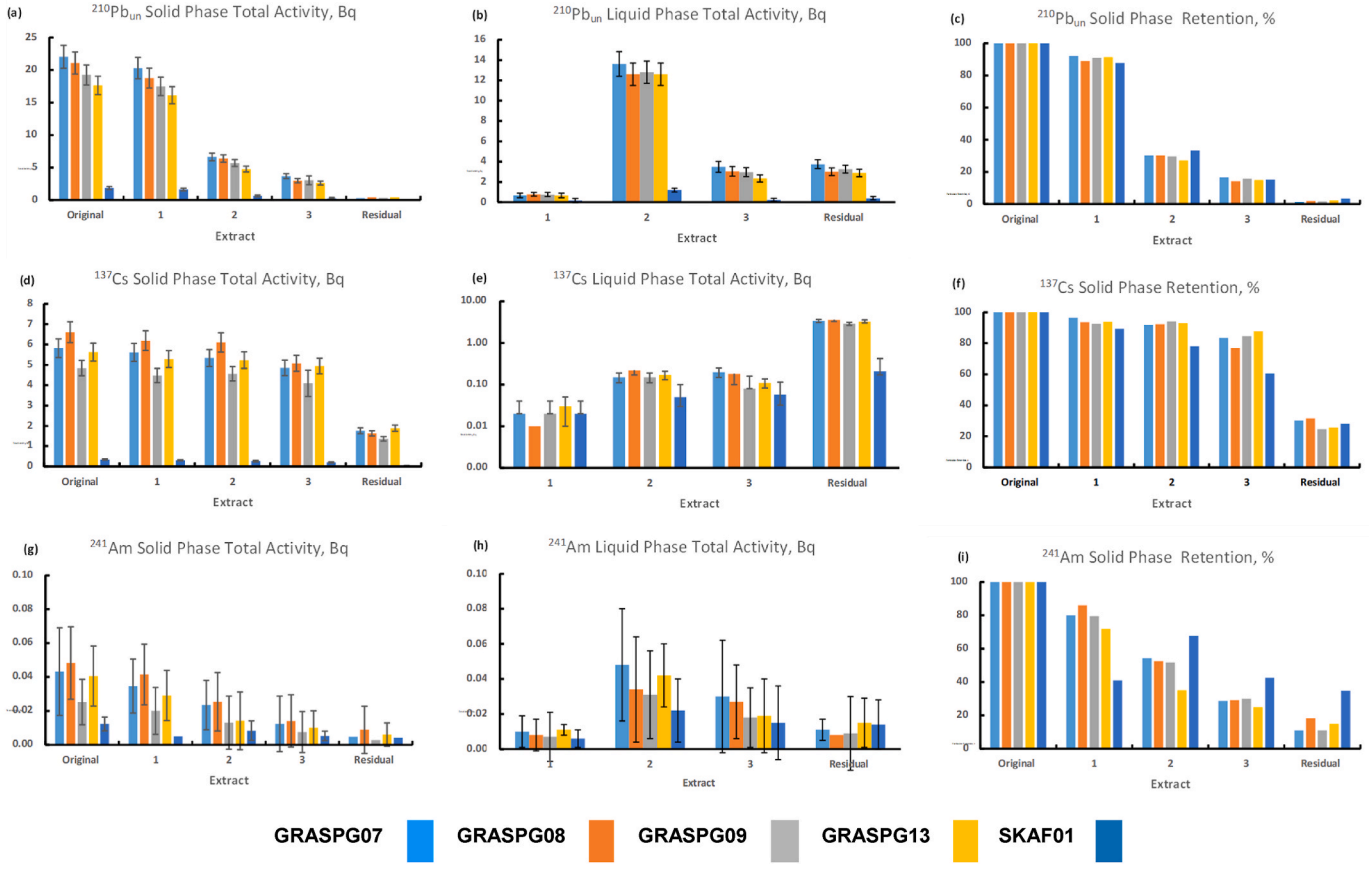

Fig. 2. Results of the 3-stage extraction of four samples of cryoconite from Sweden (GRASPGXX) and one from Iceland (SKAF01). The graphs a, d and g show the activities (Bq) of the radionuclides ^{210}Pb$_{un}$, ^{137}Cs and ^{241}Am prior to, and after, extractions; graphs b, e and h show the activities of the radionuclides in the four liquid extracts; graphs c, f and i show the percentage particulate retention of the radionuclides following extraction by the sequential digests.

5. Discussion

5.1. Chemical extractability of fallout radionuclides on cryoconites

Application of the BCR sequential extraction procedure allowed quantification of the remobilisation of FRNs from specific sorption sites on cryoconite particles, thereby giving an insight into FRN associations with various solid phases. Radionuclides desorbed in the first stage are classed as weakly bound to cation exchange sites and are, therefore, chemically labile. The second stage involves the release of radionuclides specifically bound to ferromanganese oxides which tend to dissolve under sub-oxic environmental conditions. Stage 3 of the selective extractions targets organic or sulphide-bound elements which are mobilised usually by the decomposition of organic matter and exposure to oxidising conditions. The residual phase consists of elements that are, in some cases, irreversibly adsorbed and may be only partially desorbed by concentrated acid.

The percentage of $^{210}Pb_{un}$ extracted as easily exchangeable was of the order of a few percent for all cryoconite samples. This result coheres with extraction experiments carried out on freshwater sediments, where 3.1% of total stable Pb was easily exchangeable (Nowrouzi et al., 2014). However, the majority of $^{210}Pb_{un}$ in cryoconite was extracted in the reducible phase (stage 2) with a mean percentage loss of ~60% across the samples (Fig. 2). This chemical fractionation implies the released $^{210}Pb_{un}$ was potentially attached to ferromanganese oxides that dissolve under anoxic reducing conditions (Zimmerman and Weindorf, 2010). A significant fraction of the remaining $^{210}Pb_{un}$, ~30%, was found in the in the oxidisable fraction (stage 3). Because of the significance of $^{210}Pb_{un}$ loss in the reducible stage, the results suggest that the samples may become more mobile under more frequent melting, leading to potential risks to the local environment.

For ^{137}Cs there are relatively minor releases in stages 1, 2, and 3, with a significant quantity remaining in the residual phase, possibly due to ^{137}Cs being bound within the crystalline structures of primary and secondary minerals. The release of ^{137}Cs from Chernobyl soils, under similar reaction conditions to those used here, was broadly similar, particularly in that ^{137}Cs was preferentially released after dosing with concentrated acid or was retained in the residual phase (Skipperud and Salbu, 2015). There was considerable variability in the extent to which ^{241}Am was released, particularly in the reducible and oxidized fractions, although with larger errors associated with activity concentrations (Fig. 2). The presence of ^{241}Am in the environment is not solely a consequence of original fallout but rather of ^{241}Pu (half-life 14.35 years) undergoing successive neutron capture events in nuclear weapons and nuclear reactors. This partially explains why global fallout is a significant contributor to the occurrence of ^{241}Am. Unlike ^{137}Cs, ^{241}Am activity is increasing in the environment due to the relatively short half-life of ^{241}Pu, with the quantity produced from Chernobyl fallout expected to reach a maximum around 2050.

5.2. Implications of fallout radionuclide mobilisation

The activity concentrations of FRNs currently stored in cryoconite on glaciers may not pose a substantial direct threat to glacial environments, however their remobilisation may cause a secondary pollution risk to aquatic systems and living species through downstream accumulation. Communities that are solely reliant on glacier meltwater could potentially have higher risks compared to those dependent solely on precipitation and glacially-fed rivers (Łokas et al., 2018). These ecosystems are, therefore, vulnerable to risks to fauna, for example, through consumption of contaminated water and vegetation, such as lichens which are known to be accumulators of radionuclides from the surrounding environment (Biazrov 1994). Since the 1960s, reindeer herding, which involves about 34% of Swedish territory, has been especially susceptible to radiocaesium contamination, mostly because of lichen consumption (Skuterud and Thørring, 2021). Since reindeer meat is a staple part of the diet of some Arctic communities it could represent a significant source of radiocaesium in indigenous northern diets (Åhman et al., 2001, Åhman, 2007). Furthermore, muscle tissues of both ringed and grey seals in the Baltic examined for ^{137}Cs following the Chernobyl accident were found to contain elevated activity concentrations, up to 250 Bq kg^{-1}, supporting the potential for ^{137}Cs bioaccumulation in the marine food web (Saremi et al., 2018). The release of contaminants from marine-terminating glaciers may thus also be a focus of future research.

Elsewhere, the concentrations of FRNs in cryoconite from a Canadian glacier (Owens et al., 2019) were below the upper threshold value of sediment quality guideline values for the protection of freshwater aquatic systems, implying the release of impurities into the proglacial ecosystem will likely have very low impact for local fauna. However, an improved understanding is required of the migration of radionuclide contaminants via aquatic systems, beyond their immediate proximity to glaciers. Uptake by flora (Lettner et al., 2006) in the Gastein Valley, Austria showed differences in ^{137}Cs uptake by various forms of vegetation, with activity concentrations reaching 4052 Bq kg^{-1}, especially at higher altitudes. These activity concentrations of ^{137}Cs demonstrate the ability of vegetation to take up FRNs, creating additional transfer pathways into the food chain. Values of ^{137}Cs recorded in cryoconite on Isfallsglaciären, Sweden were also exceptional, reaching a maximum of 4533 ± 350 Bq kg^{-1}, however values recorded in proglacial sediments were at least an order of magnitude lower (Clason et al., 2021). Due to the existing ^{137}Cs load in soils, however, it has been speculated that locations with past ^{137}Cs contamination may increase its transmission within the food chain should future contamination episodes occur (Åhman et al., 2001).

Whilst the concentrations of ^{241}Am in our study were close to the detection limit, even small levels ingested into the body in a soluble form can cause significant health hazards. Intake of ^{241}Am into the body may concentrate in the skeleton, muscles, and liver, remaining for decades and exposing the body tissues to both alpha and gamma radiation, thereby increasing the risk of developing cancer (Xiao et al., 2014). The contamination risk may not be an immediate concern for glacial environments and their ecosystems, but ongoing glacier retreat and release of stored contaminants could result in a gradual accumulation of the toxicity of remobilized FRNs in proglacial lakes and sediments (Pavlova et al., 2015).

5.3. Implications of glacier retreat for contaminant mobilisation

It is predicted that about 80% of glaciers in the European Alps, and 30% of glaciers in Alaska may disappear by the end of the 21st century (Huss et al., 2017), with a similar picture for mountain glacier regions globally. Furthermore, significant changes in glacier runoff have been predicted over various timescales within glacier drainage basins worldwide by Huss and Hock (2018), who concluded that peak melt water had already been reached in 45% of the basins examined, with glacial runoff predicted to maintain an increase beyond 2050 in many cases. As glaciers approach peak water production, it is anticipated that remobilisation of trapped glacial contaminants will continue for decades or more and may increase. For example, Chen et al. (2019) demonstrated a strong correlation between contaminant release fluxes and glacial melt intensity in the Tibetan Plateau, while glacial melt and precipitation have driven the expansion of lakes in the region. There is currently a very limited understanding of the total inventory of FRNs within cryoconite deposits, so further work is required to assess the potential risk of FRN mobilization and downstream deposition in line with glacier retreat. Furthermore, although retreat of glaciers, and associated fluxes of sediments and contaminants, might primarily impact the organisms found in proximal rivers and lakes, future research is needed to investigate the potential risks of gradual FRN accumulation in proglacial environments.

6. Conclusion

Our study confirms that cryoconite accumulates high activity concentrations of FRNs which have varying degrees of chemically induced availability. The original FRN activity concentrations were considerably higher in samples from Sweden than Iceland, and orders of magnitude above local background levels in the Isfallsglaciären proglacial catchment, with activities up to up to 3300 Bq kg^{-1} for ^{137}Cs, 10,950 Bq kg^{-1} for $^{210}Pb_{un}$, and 24.1 Bq kg^{-1} for ^{241}Am. The majority of $^{210}Pb_{un}$ in cryoconite samples was extracted in the reducible phase, suggesting potential for increased mobilization under higher melt scenarios. A significant portion of ^{137}Cs remained in the residual phase, while there was large variability in the release of ^{241}Am at different stages and between samples. These findings are important because we now understand that FRN accumulation is commonplace in cryoconite found in glaciers across the global cryosphere, and the results of this study imply a relationship between the chemical mobility of FRNs and downstream transportation and potential contamination. The chemical availability of radionuclides in cryoconite thus requires further investigation, particularly the examination of the release of radioactive contaminants from cryoconite under a variety of chemical conditions, especially those mimicking conditions of radionuclide desorption when cryoconite encounters animal or human gastro-intestinal digestive processes. Future experiments could focus on the release of contaminants from cryoconite during uptake by glacial and proglacial biota and, importantly, through the ingestion of cryoconite-contaminated drinking water by fauna. Furthermore, future work should also examine the contribution of FRNs to contamination risk in glacial regions under scenarios of increased melt and proglacial lake evolution. Smaller glaciers in increasingly warm settings are likely to be more vulnerable to rapid release of materials currently stored in snow, ice, and glacial sediments, and the work presented here highlights the importance of investigating areas where secondary contamination could directly affect local communities and ecosystems that rely on glacier water in near-source, high-latitude, and high-altitude regions.

Declaration of competing interest

The authors declare the following financial interests/personal relationships which may be considered as potential competing interests: Caroline Clason reports financial support was provided by INTERACT. Caroline Clason reports financial support was provided by the Quaternary Research Association.

Data availability

All data are provided within the article and supplementary materials

Acknowledgements

Sample collection in Sweden and Iceland was supported by INTERACT Transnational Access and Quaternary Research Association funding respectively, awarded to CC. We thank Nick Selmes and Ralph Fyfe for support in the field.

Appendix A. Supplementary data

Supplementary data to this article can be found online at https://doi.org/10.1016/j.jenvrad.2023.107260.

References

Åhman, B., Åhman, G., 1994. Radiocesium in Swedish reindeer after the Chernobyl fallout: seasonal variations and long-term decline. Health Phys. 66, 503–512. https://doi.org/10.1097/00004032-199405000-00002.

Åhman, B., 2007. Modelling radiocaesium transfer and long-term changes in reindeer. J. Environ. Radioact. 98, 153–165. https://doi.org/10.1016/j.jenvrad.2006.11.011.

Åhman, B., Wright, S., Howard, B., 2001. Effect of origin of radiocaesium on the transfer from fallout to reindeer meat. Sci. Total Environ. 278, 171–181. https://doi.org/10.1016/S0048-9697(01)00646-5.

Baccolo, G., Nastasi, M., Massabò, D., Clason, C., Di Mauro, B., Di Stefano, E., Łokas, E., Prati, P., Previtali, E., Takeuchi, N., Delmonte, B., Maggi, V., 2020a. Artificial and natural radionuclides in cryoconite as tracers of supraglacial dynamics: insights from the Morteratsch glacier (Swiss Alps). Catena 191, 104577. https://doi.org/10.1016/j.catena.2020.104577.

Baccolo, G., Łokas, E., Gaca, P., Massabò, D., Ambrosini, R., Azzoni, R.S., Clason, C., Di Mauro, B., Franzetti, A., Nastasi, M., Prata, M., Prati, P., Previtali, E., Delmonte, B., Maggi, V., 2020b. Cryoconite: an efficient accumulator of radioactive fallout in glacial environments. Cryosphere 14, 657–672. https://doi.org/10.5194/tc-14-657-2020.

Bagshaw, E.A., Tranter, M., Fountain, A.G., Welch, K., Basagic, H.J., Lyons, W.B., 2013. Do cryoconite holes have the potential to be significant sources of C, N, and P to downstream depauperate ecosystems of Taylor Valley, Antarctica? Arctic Antarct. Alpine Res. 45, 440–454. https://doi.org/10.1657/1938-4246-45.4.440.

Beard, D.B., Clason, C.C., Rangecroft, S., Poniecka, E., Ward, K.J., Blake, W.H., 2022a. Anthropogenic contaminants in glacial environments 1: inputs and accumulation. Prog. Phys. Geogr. 46, 630–648. https://doi.org/10.1177/03091333221107376.

Beard, D.B., Clason, C.C., Rangecroft, S., Poniecka, E., Ward, K.J., Blake, W.H., 2022b. Anthropogenic contaminants in glacial environments II: release and downstream consequences. Prog. Phys. Geogr. 46, 630–648. https://doi.org/10.1177/03091333221127342.

Biazrov, L., 1994. The radionuclides in lichen thalli in Chernobyl and East Urals areas after nuclear accidents. Phyton 34, 85–94. https://doi.org/10.1657/15230430(2004)036[0502:AMASTA]2.0.CO:2.

Buda, J., Łokas, E., Pietryka, M., Richter, D., Magowski, W., Iakovenko, N.S., Porazinska, D.L., Budzik, T., Grablec, M., Grzesiak, J., Klimaszyk, P., Gaca, P., Zawierucha, K., 2020. Biotope and biocenosis of cryoconite hole ecosystems on Ecology Glacier in the maritime Antarctic. Sci. Total Environ. 724, 138112 https://doi.org/10.1016/j.scitotenv.2020.138112.

Cauvy-Fraunié, S., Dangles, O., 2019. A global synthesis of biodiversity responses to glacier retreat. Nature Ecology & Evolution 3, 1675–1685. https://doi.org/10.1038/s415501-0189-1042-8.

CCME, 1995. Canadian Council of Ministers of the Environment. Canadian Sediment Quality Guidelines for the Protection of Aquatic Life. CCME EPC -98E, Summary Tables. Environment Canada, Winnipeg, Canada, pp. 1–5.

Chen, M., Chanfei, W., Xiaoping, W., et al., 2019. Release of perfluoroalkyl substances from melting glacier of the Tibetan Plateau: insights into the impact of global warming on the cycling of emerging pollutants. J. Geophys. Res. 124, 7442–7456. https://doi.org/10.1029/2019JD030566.

Clason, C.C., Blake, W.H., Selmes, N., Taylor, A., Boeckx, P., Kitch, J., Mills, S.C., Baccolo, G., Millward, G.E., 2021. Accumulation of legacy fallout radionuclides in cryoconite on Isfallsglaciären (Arctic Sweden) and their downstream spatial distribution. Cryosphere 15, 5151–5168. https://doi.org/10.5194/tc-15-5151-2021.

Clason, C.C., Baccolo, G., Łokas, E., Owens, P.N., Wachniew, P., Millward, G.E., Taylor, A., Blake, W.H., Beard, D.B., Poniecka, E., Selmes, N., Bagshaw, E.A., Cook, J., Fyfe, R., Hay, M., Land, D., Takeuchi, N., Nastasi, M., Sisti, M., Pittino, F., Franzetti, A., Ambrosini, R., Di Mauro, B., 2023. Global variability and controls on the accumulation of fallout radionuclides in cryoconite. Sci. Total Environ. 894, 164902 https://doi.org/10.1016/j.scitotenv.2023.164902.

Cook, J., Edwards, A., Takeuchi, N., Irvine-Finn, T., 2016. Cryoconite: the dark biological secret of the cryosphere. Prog. Phys. Geogr. 40, 66–111. https://doi.org/10.1177/0309133315616574.

Corcho Alvarado, J.A., Steinmann, P., Estier, S., Bochud, F., Haldimann, M., Froidevaux, P., 2014. Anthropogenic radionuclides in atmospheric air over Switzerland during the last few decades. Nat. Commun. 5, 3030. https://doi.org/10.1038/ncomms:1030(2014).

Ferrario, C., Finizio, A., Villa, S., 2017. Legacy and emerging contaminants in meltwater of three Alpine glaciers. Sci. Total Environ. 574, 350–357. https://doi.org/10.1016/j.scitotenv.2016.09.067.

Franz, T.P., Eisenreich, S.J., 1998. Snow scavenging of polychlorinated biphenyls and polycyclic aromatic hydrocarbons in Minnesota. Environ. Sci. Technol. 32, 1771–1778. https://doi.org/10.1021/es970601z.

Gadd, G., 1996. Influence of microorganisms on the environmental fate of radionuclides. Endeavour 20, 150–156. https://doi.org/10.1016/S0160-9327(96)10021-1.

Grannas, A.M., Bogdal, C., Hageman, K.J., Halsall, C., Harner, T., Hung, H., Kallenborn, R., Klán, P., Klánová, J., MacDonald, R.W., Meyer, T., Wania, F., 2013. The role of the global cryosphere in the fate of organic contaminants. Atmos. Chem. Phys. 13, 3271–3305. https://doi.org/10.5194/acp-13-3271-2013.

Herbert, B.M.J., Villa, S., Halsall, C.J., 2006. Chemical interactions with snow: understanding the behavior and fate of semi-volatile organic compounds in snow. Ecotoxicol. Environ. Saf. 63, 3–16.

Huss, M., Hock, R., 2018. Global-scale hydrological response to future glacier mass loss. Nat. Clim. Change 8, 135–140. https://doi.org/10.1038/s41558-017-0049-x.

Huss, M., Bookhagen, B., Huggel, C., Jacobsen, D., Bradley, R.S., Clague, J.J., et al., 2017. Toward mountains without permanent snow and ice. Earth Future 5, 418–435. https://doi.org/10.1002/2016EF000514.

Jiao, X., Dong, Z., Baccolo, G., Fangzhou, L., Wei, T., Jing, L., Qin, X., 2023. Insights on the distribution and environmental implications of the radio-isotope 235U in surface soils and glaciers of the Tibetan Plateau. Environ. Pollut. 317, 120824 https://doi.org/10.1016/j.envpol.2022.120624.

Kenna, T.C., 2009. Using sequential extraction techniques to assess the partitioning of plutonium and neptunium-237 from multiple sources in sediments from the Ob River

(Siberia). J. Environ. Radioact. 100, 547–557. https://doi.org/10.1016/j.jenrad.2009.03.016.

Lettner, H., Griesebner, A., Peer, T., Hubmer, A.K., Pintaric, M., 2006. Altitude dependent ^{137}Cs concentrations in different plant species in Alpine agricultural areas. J. Environ. Radioact. 86, 12–30. https://doi.org/10.1016/j.jenvrad.2005.06.007.

Łokas, E., Zawierucha, K., Cwanek, A., Szufa, K., Gaca, P., Mietelski, J., Tomankiewicz, E., 2018. The sources of high airborne radioactivity in cryoconite holes from the Caucasus (Georgia). Sci. Rep. 8, 10802 https://doi.org/10.1038/s41598-018-29076-4.

Marren, P.M., Toomath, S.C., 2014. Channel pattern of proglacial rivers: topographic forcing due to glacier retreat. Earth Surf. Process. Landforms 39 (7), 943–951. https://doi.org/10.1002/esp.3545.

Mietelski, J.W., 2002. Radionuclides from Chernobyl hot particles in the environment of North-Eastern Poland - a leaching experiment. Radioprotection-Colloques 37. C1-249-C1254.

Milner, A., Khamis, K., Battin, T., Brittain, J., Barrand, N., Füreder, L., Cauvy-Fraunié, S., Gíslason, G., Jacobsen, D., Hannah, D., Hodson, A., Hood, E., Lencioni, V., Ólafsson, J., Robinson, C., Tranter, M., Brown, L., 2017. Glacier shrinkage driving global changes in downstream systems. Proc. Natl. Acad. Sci. USA 114, 9770–9778. https://doi.org/10.1073/pnas.1619807114.

Nowrouzi, M., Pourkhabbaz, A., Rezaei, M., 2014. Sequential extraction analysis of metals in sediments from the hara biosphere reserve of southern Iran. Chem. Speciat. Bioavailab. 26, 273–277. https://doi.org/10.3184/095422914X14141630849689.

Owens, P., Blake, W., Millward, G., 2019. Extreme levels of fallout radionuclides and other contaminants in glacial sediment (cryoconite) and implications for downstream aquatic ecosystems. Sci. Rep. 9, 12531 https://doi.org/10.1038/s41598-019-48873-z.

Owens, P.N., Stott, T.A., Blake, W.H., Millward, G.E., 2023. Legacy radionuclides in cryoconite and proglacial sediment on orwell glacier, signy island, Antarctica. J. Environ. Radioact. 264, 107206 https://doi.org/10.1016/j.jenvrad.2023.107206.

Pawlak, F., Koziol, K., Polkowska, Z., 2021. Chemical hazard in glacial melt? The glacial system as a secondary source of POPs (in the Northern Hemisphere). A systematic review. Sci. Total Environ. 778, 145244 https://doi.org/10.1016/j.scitotenv.2021.145244.

Pavlova, P., Zennegg, M., Anselmetti, F., Schmid, P., Bogdal, C., Steinlin, C., Jäggi, M., Schwikowski, M., 2015. Release of PCBs from Silvretta glacier (Switzerland) investigated in lake sediments and meltwater. Environ. Sci. Pollut. Control Ser. 23, 10308–10316. https://doi.org/10.1007/s11356-015-5854-z.

Pueyo, M., Rauret, G., Lück, D., Yli-Halla, M., Muntau, H., Quevauviller, P., López-Sánchez, J., 2001. Certification of the extractable contents of Cd, Cr, Cu, Ni, Pb and Zn in a freshwater sediment following a collaboratively tested and optimised three-step sequential extraction procedure. J. Environ. Monit. 3, 243–250. https://doi.org/10.1039/b010235k.

Saremi, S., Isaksson, M., Harding, K., 2018. Bio-accumulation of radioactive caesium in marine mammals in the Baltic Sea – reconstruction of a historical time series. Sci. Total Environ. 631–632, 7–12. https://doi.org/10.1016/j.scitotenv.2018.02.282.

Skipperud, L., Salbu, B., 2015. Sequential extraction as a tool for mobility studies of radionuclides and metals in soils and sediments. Radiochim. Acta 103, 187–197. https://doi.org/10.1515/ract-2014-2342.

Skuterud, L., Pedersen, Ø., Staaland, H., Røed, K.H., Salbu, B., Liken, A., Hove, K., 2004. Absorption, retention and tissue distribution of radiocaesium in reindeer: effects of diet and radiocaesium source. Radiat. Environ. Biophys. 43, 293–301. https://doi.org/10.1007/s00411-004-0257-4.

Skuterud, L., Thørring, H., 2021. Caesium-137 in mountain flora with emphasis on reindeer's diet – spatial and temporal trends. J. Environ. Radioact. 231, 106551 https://doi.org/10.1016/j/jenvrad.2021.106551.

Smith, N., 1978. Sedimentation processes and patterns in a glacier-fed lake with low sediment input. Can. J. Earth Sci. 15, 741–756. https://doi.org/10.1139/e78-081.

Stefánsson, H., Peternell, M., Konrad-Schmolke, M., et al., 2021. Microplastics in glaciers: first results from the Vatnajökull ice cap. Sustainability 13, 4183. https://doi.org/10.3390/su13084183.

Taylor, A., Blake, W., Couldrick, L., Keith-Roach, M.J., 2012. Sorption behaviour of beryllium-7 and implications for its use as a sediment tracer. Geoderma 187–188, 16–23. https://doi.org/10.1016/j.geoderma.2012.04.013.

Tieber, A., Lettner, H., Bossew, P., Hubmer, A., Sattler, B., Hofmann, W., 2009. Accumulation of anthropogenic radionuclides in cryoconites on Alpine glaciers. J. Environ. Radioact. 100, 590–598. https://doi.org/10.1016/j.jenvrad.2009.04.008.

Wedepohl, K.H., 1995. The composition of the continental crust. Geochimica Cosmochimca Acta 59, 1217–1232.

Wilflinger, T., Lettner, H., Hubmer, A., Bossew, P., Sattler, B., Slupetzky, H., 2018. Cryoconites from Alpine glaciers: radionuclide accumulation and age estimation with Pu and Cs isotopes and 210 Pb. J. Environ. Radioact. 186, 90–100. https://doi.org/10.1016/j.envrad.2017.06.020.

Xiao, G., Saunders, D., Jones, R., Caldwell, K., 2014. Determination of 241Am in urine using sector field inductively coupled plasma mass spectrometry (SF-ICP-MS). J. Radioanal. Nucl. Chem. 301 (1), 285–291.

Zawierucha, K., Buda, J., Pietryka, M., Richter, D., Łokas, E., Lehmann-Konera, S., Makowska, N., Bogdziewicz, M., 2017. Snapshot of micro-animals and associated biotic and abiotic environmental variables on the edge of the south-west Greenland ice sheet. Limnology 19, 141–150. https://doi.org/10.1007/s10201-017-0528-9.

Zimmerman, A.J., Weindorf, D.C., 2010. Heavy metal and trace metal analysis in soil by sequential extraction: a review of procedures. Int. J. Anal. Chem. 2010, 387803 https://doi.org/10.1155/2010/387803.